

NASA-CR-197370

**CORONAGRAPHIC OBSERVATIONS AND ANALYSES  
OF THE ULTRAVIOLET SOLAR CORONA**

NASA Grant      NAG5-613

**Semiannual** Status Report Nos. 21, 22, 23, and 24

**Period 1** October 1992 to 30 September 1994

N95-20558

Unclas

G3/92 0041109

Principal Investigator

Dr. John L. Kohl

Prepared for  
National Aeronautics and Space Administration  
Wallops Island, VA 23337

Smithsonian Institution  
Astrophysical Observatory  
Cambridge, MA 02138

The Smithsonian Astrophysical Observatory  
is a member of the  
Harvard-Smithsonian Center for Astrophysics

(NASA-CR-197370) CORONAGRAPHIC  
OBSERVATIONS AND ANALYSES OF THE  
ULTRAVIOLET SOLAR CORONA Semiannual  
Status Report Nos. 21, 22, 23, and  
24, 1 Oct. 1992 - 30 Sep. 1994  
(Smithsonian Astrophysical  
Observatory) 14 p

The NASA Technical Officer for this grant is Mr. Larry J. Early, Code 840.0, Goddard  
Space Flight Center/Wallops Flight Facility, Wallops Island, VA 23337.

IN-92-ER  
0017  
41109  
14P



## Introduction

This status report for the period 1 October 1992 to 30 September 1994 covers the final preparation and first observations with the Spartan Ultraviolet Coronal Spectrometer on Spartan 201-1, and the preparation and second flight for Spartan 201-2. Both flights were fully successful and resulted in high quality spectroscopic observations of the extended solar corona out to 3.5 solar radii from Sun-center. The primary focus of this report is the results from Spartan 201-1. There is also a brief description of the evaluation of the quick look data from the second flight. Highlights from the first flight include a discovery that the proton velocity distribution in coronal holes is complex and consists of a central core with elevated high velocity wings compared to a Gaussian shape. Polar plumes were also found to have enhanced high velocity fractions, but they were found to have a narrower core velocity distribution compared to coronal hole observations at the same projected radial height. Spartan 201-1 also produced the first measurements of proton velocity distributions in helmet streamers. A Doppler dimming analysis of the combined white light polarization brightness and HI Ly- $\alpha$  observations is being carried out for a coronal region extending from the observed southwest helmet streamer into the south polar coronal hole. The preliminary indication is that the bulk outflow velocity is large enough at 2 solar radii from Sun-center to cause Doppler dimming (i.e., greater than 150 km/s). Spartan 201-1 also provided an observation of a CME with an apparent velocity of about 200 km/s. The CME caused about a 10 percent increase in the visible polarization brightness behind its leading edge. Observations before and during the CME indicated that the HI Ly- $\alpha$  intensity did not change by more than 20%. This is the first ultraviolet observation of a CME. The analysis of the CME observation is ongoing.

The following presentations and publications have been produced as a result of Spartan Mission 201-1.

List of Talks and Publications:

- *Ultraviolet Coronal Spectrometer Observations During Spartan Mission 201-1*, L.D. Gardner, S. Fineschi, D. Hassler, M. Romoli, L. Strachan, and J.L. Kohl, 1993, Bull. AAS, 25,1200.
- *Ultraviolet Spectroscopic Observations of Polar Coronal Holes During Spartan Mission 201-1*, J.L. Kohl, L.D. Gardner, D. Hassler, and L. Strachan, 1993, Bull. AAS, 25,1209.
- *Ultraviolet Spectroscopic Observations of a Helmet Streamer During Spartan Mission 201-1*, L. Strachan, L.D. Gardner, D. Hassler, and J.L. Kohl, 1993, Bull. AAS, 25,1209.
- *Radiometric Calibration of UVCS/SOHO and UVC/Spartan*, L. Strachan, L.D. Gardner, D.M. Hassler, J.L. Kohl, S. Fineschi, and M. Romoli, 1993, Proceedings

of the Ninth Workshop on the Vacuum Ultraviolet Calibration of Space Experiments, Boulder, Colorado.

- *Spectroscopic Observations of a Helmet Streamer During Spartan Mission 201-1*, L. Strachan, L.D. Gardner, D. Hassler, and J.L. Kohl, 1993, EOS, Transactions, AGU, Suppl., 74, no. 43, 496.
- *The Spartan Ultraviolet Coronal Spectrometer*, L.D. Gardner, J.L. Kohl, L. Strachan, and D.M. Hassler, 1993, Bull. AAS 25, 1300.
- *Spartan 201 H I Lyman-Alpha Observations of a Polar Coronal Region*, J.L. Kohl, L.D. Gardner, D.M. Hassler, and L. Strachan, 1993, Bull. AAS 25, 1386.
- *Spartan 201 Observations of the Ultraviolet Extended Solar Corona*, L.D. Gardner, D.M. Hassler, L. Strachan, and J.L. Kohl, 1994, in Solar Coronal Structures, Proceedings of the 144th Col. IAU.
- *Recent Results from the Spartan 201-1 Mission and Plans for the Ulysses South Polar Passage*, L. Strachan, J.L. Kohl, and L.D. Gardner, 1994, invited talk at Univ. of Maryland Space Science Colloquium, College Park, Md.
- *UV Coronal Observations from Spartan Missions 201-1 and 201-2*, L.D. Gardner, L. Strachan, and J.L. Kohl, 1994, EOS, Transactions, AGU, Suppl., 75, no. 16, 257.
- *An Analysis of H I Ly- $\alpha$  Line Profiles in Polar Coronal Hole Regions Observed by Spartan 201*, J.L. Kohl, L.D. Gardner, and L. Strachan, 1994, EOS, Transactions, AGU, Suppl., 75, no. 16, 257.
- *Spatial Distributions of Hydrogen Kinetic Temperatures and Bulk Flow Velocities in a Coronal Streamer Observed by Spartan 201*, L. Strachan, L.D. Gardner, and J.L. Kohl, 1994, EOS, Transactions, AGU, Suppl., 75, no. 16, 276.
- *Ultraviolet Spectroscopy of the Extended Solar Corona During the Spartan 201 Mission*, J.L. Kohl, L.D. Gardner, L. Strachan, and D.M. Hassler, 1994, Space Science Reviews (in press).
- *Preliminary Results from Spartan 201: Coronal Streamer Observations*, L. Strachan, L.D. Gardner, D.M. Hassler, and J.L. Kohl, 1994, Space Science Reviews (in press).
- *The Ultraviolet Coronagraph for Spartan 201*, L.D. Gardner, J.L. Kohl, L. Strachan, H. Weiser, and D.M. Hassler, 1994 (in preparation).
- *Spartan 201 Coronal Spectroscopy During the Polar Passes of Ulysses*, J.L. Kohl, L.D. Gardner, and L. Strachan, 1994, Proc. 28th ESLAB Symposium, ESA.

- *Ly-Alpha And White Light Observations Of A CME During The Spartan 201-1 Mission*, D.M. Hassler, L. Strachan, L.D. Gardner, J.L. Kohl, M. Guhathakurta, R.R. Fisher, and K. Strong, 1994, Proceedings, 3rd SOHO Workshop (submitted).

## **Integration Of The UVCS For Spartan 201-1**

During this reporting period, the pre-flight spacecraft integration activities at GSFC were completed successfully. The Spartan 201 spacecraft passed its vibration test which was verified by a 43-hour mission simulation in October 1992. In December 1992 the Spartan spacecraft was shipped to Kennedy Space Center for testing and integration into the orbiter Discovery. This activity led to the successful flight and recovery during the month of April 1993.

After the flight, the spacecraft was returned to GSFC for rechecking the optical alignments of both the UVCS and WLC instruments. The co-registration between the instruments was checked also. The optical alignments were found to have held during the flight and were in close agreement with the pre-flight alignments.

Next the UVCS was de-integrated from the Spartan Instrument Carrier at GSFC and returned to SAO for post-flight characterization. Those activities are described in the section on the preparations for the second flight.

## **UVCS Results From Spartan 201-1**

### **Overview of Ultraviolet Spectroscopic Observations During Spartan 201-1**

Spartan 201-1 was deployed from the space shuttle on 11 April 1993 and spent about 40 hours observing the extended solar corona. The four primary targets for Spartan Mission 201-1 were the north polar corona, the south polar corona, a helmet streamer at position angle  $135^\circ$  and an active region above the west limb. Center to limb scans (from  $-8.0$  arcmin to the limb) of the HI Ly- $\alpha$  profile and the OVI intensities were made at position angles between  $281^\circ$  and  $352^\circ$ . There also were measurements of the HI Ly- $\alpha$  geocorona at five orientations between  $95^\circ$  and  $160^\circ$  from the Sun-center direction. Background measurements were made while the instrument was in the Earth's umbra and facing the Earth. In order to distinguish between a light signal and background, data were accumulated with two very different unvignetted areas of each telescope mirror.

Figure 1 indicates all of the solar spatial elements observed during the mission. Concentrating on the smallest rectangles, which indicate the HI Ly- $\alpha$  profile measurements, it can be seen that the four targets were sampled extensively, but not completely. The most complete coverages were for the helmet streamer at  $135^\circ$  and for the south polar region.

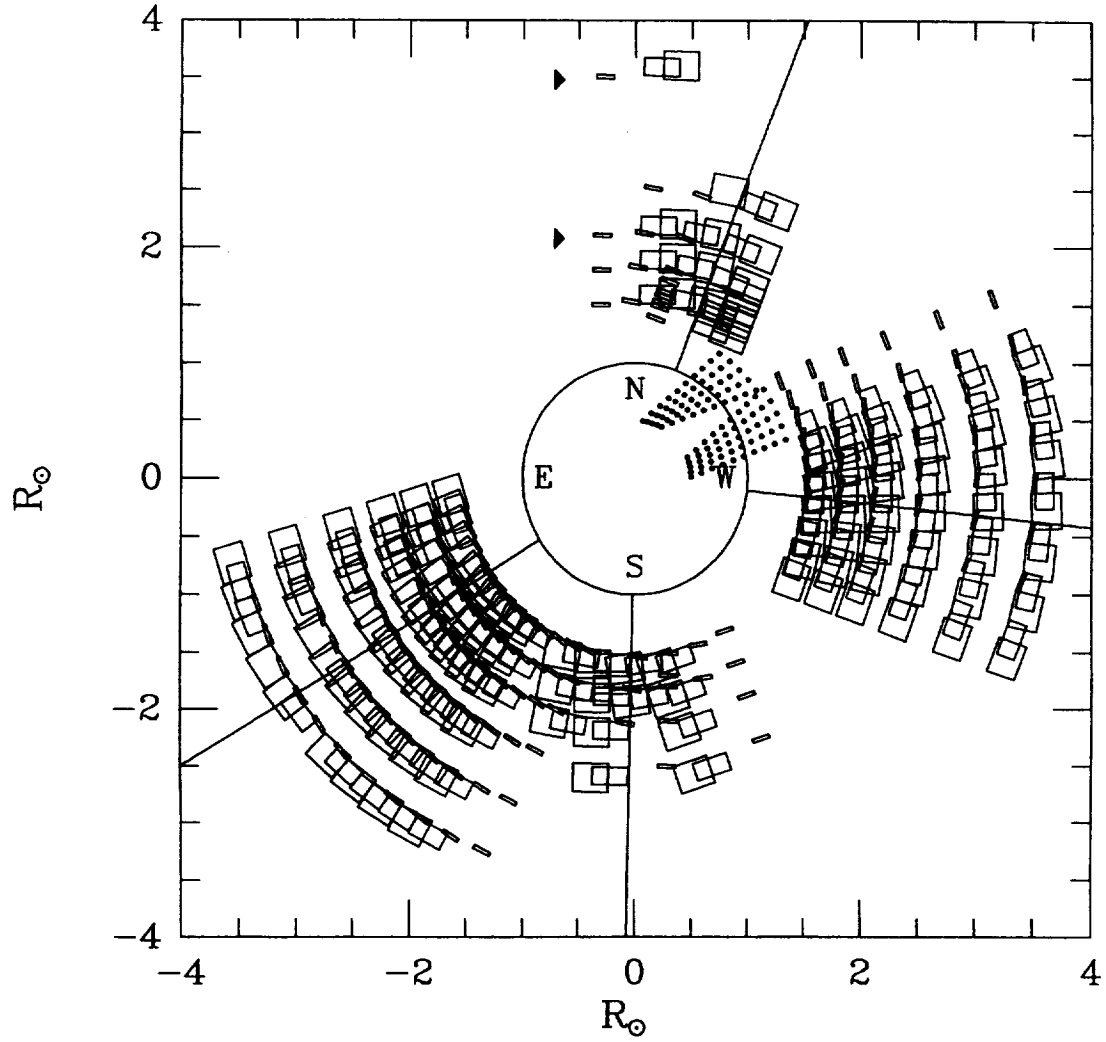


Figure 1: Spatial elements observed by the Ultraviolet Coronal Spectrometer during the Spartan 201-1 mission are illustrated. At any instant, the instrument observes three spatial elements (e.g., the group of three rectangles at the extreme top of the figure). The smallest and largest rectangles are, respectively, for observations of the line profile and integrated line intensity of HI Ly- $\alpha$ , and the intermediate sized one is for the intensity of OVI lines. Telescope motions are used to vary the heliocentric height and the entire spacecraft is rotated to vary the position angle.

Observations by the Spartan White Light Coronagraph indicate that the north and south polar regions are coronal holes with substructures consisting of polar plumes or rays that extend outward to heliocentric heights in excess of  $5 R_{\odot}$  (Guhathakurta, *et al.* 1994).

### **Inflight Instrument Performance**

The initial evaluation of the in-flight performance was based, primarily, on the observations at  $3.52 R_{\odot}$  in the north polar hole, the geocorona observation at  $95^{\circ}$  to the Sun, and the background measurements in the Earth's umbra. Inflight performance was also inferred from the preflight and post-flight calibrations.

In the case of radiometric sensitivity, the laboratory calibrations indicated that the instrument retained its sensitivity during the mission.

The spectral resolution profile was checked by observing the geocoronal Ly- $\alpha$  line (see Figure 2). The actual linewidth is expected to be much narrower than the instrument, and so the measured profile is indicative of the instrument's response to monochromatic light. The full width at half maximum (FWHM) is 0.027 nm.

An upper limit on the stray light levels during the mission can be estimated by comparing the shape of the HI Ly- $\alpha$  profile from the disk to the observation of the north polar hole at  $3.5 R_{\odot}$ . The latter consists of a narrow component attributable, primarily, to the geocorona, and a broader coronal component. Stray light is expected to be due to scattering of solar disk light in the instrument. It would therefore have the spectral line shape of the solar disk as measured with the Spartan instrument, which has a line width that is between that of the observed narrow and broad components. By comparing the two profiles it is clear that the stray light level is small compared to the observed coronal intensities.

The background count rate during the mission was determined in two ways. One approach was to collect data while the instrument was in the Earth's umbra and pointed toward the Earth's surface. In that case, measurements were made with two different mirror areas exposed, a relatively small area and a much larger area. The detector background was separated from detected photons by making use of the fact that the photon signal scaled with the unvignetted area and the background did not. The other method was based on the count rate in the far line wings. Laboratory data were used to relate the background in the central pixels to that in the line wing. It was also necessary to correct the data for cross talk using laboratory data. Both techniques indicated that the average background per pixel was about 0.013 counts per second.

### **Observations of the North Polar Coronal Hole During Spartan 201-1**

The North polar coronal hole was observed at three orientations. There were observations at about 1.5, 1.8, 2.1, 2.5, 3.0, and 3.5 solar radii from Sun-center.

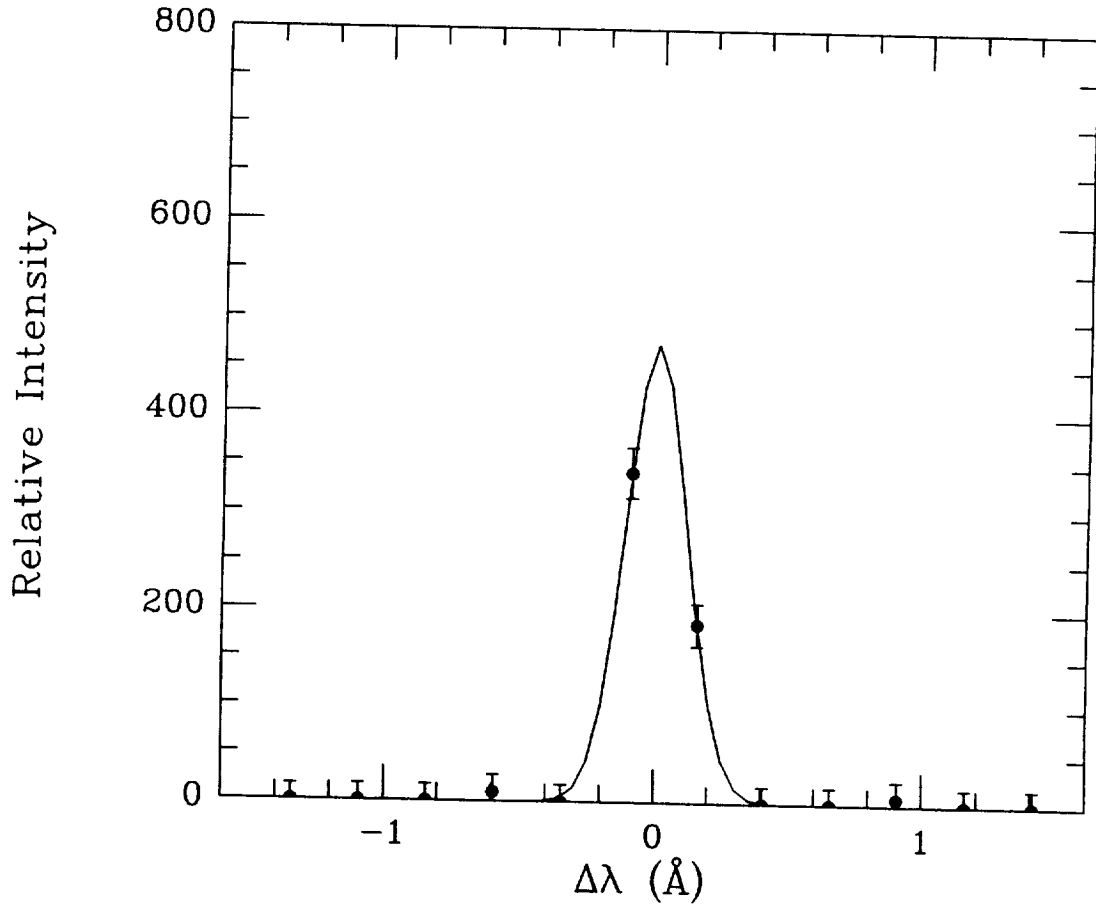


Figure 2: The geocoronal HI Ly- $\alpha$  line observed in the Earth's umbra. Since the geocoronal line is much narrower than the instrument resolution profile, it provides an in-flight measurement of the spectral resolution.



The observation at  $2.13 R_{\odot}$  appears to consist of at least three components. The geocoronal component is expected to have a width that is essentially identical to the instrument profile and can be easily identified. The remainder of the profile cannot be fit with a simple Gaussian curve such as that to be expected for a purely thermal and spherically symmetric corona. It appears instead that the profile consists of a central portion with a Doppler half width of about 0.040 nm, which corresponds to a proton kinetic temperature of about  $5.8 \times 10^5$  K and broad line wings. If you treat the line wings as a separate component, the best fit is for a Doppler half width of about 0.091 nm which corresponds to a proton kinetic temperature of about  $3.0 \times 10^6$  K.

Observations at about the same position angle and at heights of 1.5 and 1.8  $R_{\odot}$  also exhibit enhanced line wings and a line core. The line core has a half width corresponding to a proton kinetic temperature of about  $8.3 \times 10^5$  K at 1.5  $R_{\odot}$  and  $1.03 \times 10^6$  K at 1.8  $R_{\odot}$ .

Several possibilities for explaining the complex shapes of the observed profiles are being investigated. In addition to a deeper analysis of the present data, this involves an analysis of Yohkoh observations and several ground based observations of the north polar region.

The explanations for the observed line shapes fall into four general categories. One possibility is that one of the coronal components results from a foreground or background structure, and the other from the coronal hole itself. For example, the narrow component which has a kinetic temperature of about  $8.3 \times 10^5$  K at 1.5  $R_{\odot}$  and  $5.8 \times 10^5$  at 2.1  $R_{\odot}$ , may be from the coronal hole, and the broader component from a foreground or background structure. Synoptic observations by Yohkoh and ground observations of the Fe XIV green line (530.3 NM) (Esser, 1993) may provide evidence for the existence of these structures. However, any such explanation must consider the reduction in the neutral hydrogen density and hence H I Ly- $\alpha$  intensity that would result from the ionization balance in a plasma with a high electron temperature relative to a cooler plasma.

Another explanation is that the ray structures observed by the White Light Corona-graph may be the source of either the narrow or the broad component. In this case there would be a much different proton velocity distribution in the rays than in the surrounding coronal hole plasma. However, the electron temperatures may not be so different.

It is also possible that waves propagate through the corona and across the line-of-sight. The waves would occupy some fraction of the line-of-sight leaving the rest as undisturbed corona. Transverse wave velocities could then account for the broad components.

In the above cases, there are two separate velocity distributions from two spatially isolated regions. There are also several possibilities for accounting for the observed profile shape with a single velocity distribution. For example, one could envision a

coronal hole with a flow geometry that is highly non-radial with a bulk outflow velocity from the near side of the coronal hole that flows nearly directly at the observer while that from the other side flows nearly directly away. An explanation for the observed profile widths of the broad component at  $2.13 R_{\odot}$  would require outflow velocities of about  $200 \text{ km s}^{-1}$ . A difficulty in that explanation is that in order to explain the broad wings over a broad range of heights, the geometry must be such that the highly non-radial flows also occur over that same range of heights.

Another explanation is a non-Maxwellian velocity distribution in a predominantly single region plasma. Models of this type have been described by Scudder (1992). The general idea is that mechanisms for thermalizing the protons in the high velocity tail of the distribution are not sufficient and so the relative number of ions with high velocities becomes larger as the coronal plasma flows outward into lower density regions.

It is important to point out that the present observation is providing direct information about the hydrogen velocity distribution and probably about that of the protons. However, the electron temperature is not being measured here, although it may be possible to infer it from ionization balance modeling.

At present, all of the above explanations, and perhaps others, are in the realm of possibility. Work is currently underway to attempt to identify the most probable explanations for the observed profiles. This will require the use of a large set of coordinated ground and space based observations undertaken during the Spartan 201-1 mission.

### **Observation of the South Polar Coronal Hole During Spartan 201-1**

The south polar coronal hole was observed at four orientations. There were observations at about 1.7, 1.8, 2.1 and 2.5 solar radii from Sun-center.

In general, the HI Ly- $\alpha$  line profiles have complex shapes with enhanced line wings relative to a Gaussian curve. The possible explanations are the same as for the north polar coronal hole discussed earlier.

Comparison to images from the White Light Coronagraph indicates that the observation at 1.8 solar radii and  $210^{\circ}$  was on a polar plume and the other observations at that height appear to be between plumes.

The difference between the profile observed on the plume and the one observed in the gap between plumes is approximately attributable to the plume, assuming that the coronal hole contributions to the profiles on and off the plume are essentially identical. This assumes that the coronal hole along both lines-of-sight is nearly the same, and that the plume occupies a negligible fraction of the coronal hole along the line-of-sight. The difference profile has a complex shape with enhanced wings over a Gaussian profile. A two component fit corresponds to kinetic temperatures of  $8.9 \times 10^5$  and  $5.3 \times 10^6 \text{ K}$ . It appears that the plume has a non-Maxwellian velocity distribution or some portion of the line of sight contains material with a very high proton temperature or large

Spectral Line	Profile Res.	Line Position	Intensity Accu.	Spatial Res.
H I Ly- $\alpha$	0.25 Å	0.05 Å (12.3 km/s)	$\pm 15\%$	$0.5' \times 2.5'$
H I Ly- $\alpha$	2.0 Å	–	$\pm 15\%$	$4.0' \times 5.0'$
N V 1238	2.0 Å	–	$\pm 15\%$	$4.0' \times 5.0'$
Fe XII 1242	2.0 Å	–	$\pm 15\%$	$4.0' \times 5.0'$
Mg VI 1192	2.0 Å	–	$\pm 15\%$	$4.0' \times 5.0'$
O VI 1032	5.0 Å	–	$\pm 15\%$	$4.0' \times 5.0'$
O VI 1037	5.0 Å	–	$\pm 15\%$	$4.0' \times 5.0'$

Table 1: Observable spectroscopic quantities of the Spartan Ultraviolet Coronal Spectrometer. Observable heliocentric heights range from 1.35 to 3.5 solar radii.

transverse wave velocity. The conversion to a velocity distribution for the plume gives a rms velocity of  $137 \text{ km s}^{-1}$ . This is smaller than the coronal hole value. It is also evident that the core of the distribution is narrower. Hence, we are left with the impression that the observed polar plume is cooler than the adjacent coronal hole or has smaller non-thermal velocities, and also likewise has an rms velocity that is much larger than that found in a Maxwellian distribution with a similar core distribution.

In addition to the observations of H I Ly- $\alpha$ , the Spartan/UVCS instrument observed the intensities of the spectral lines listed in Table I. The OVI observations were affected by an apparent atmospheric absorption which may be attributable to NO or N<sub>2</sub>. Atmospheric models are being used to help explain the absorption. Attempts to account for the absorption by referencing the disk observations indicate an unexpectedly large intensity of the 1037 Å component relative to the 1032 component. A possible explanation is pumping by a neighboring CII spectral line, but this explanation requires a large (150 km/s) OVI outflow velocity within 2 solar radii of Sun-center. The observed intensities of Fe XII  $\lambda$ 1242, NV  $\lambda$ 1238, and possibly Mg VI  $\lambda$ 1192, appear to be suitable for determinations of chemical abundances at heights between 1.7 and 2.5 solar radii.

## **Southeast Streamer and Coronal Hole Edge**

Leonard Strachan has reported on the spatial distribution of hydrogen kinetic temperatures and velocities in the streamer observed on the Sun's southeast limb. These include the first measurements of hydrogen kinetic temperatures in a coronal streamer. It was found that the radial distribution of kinetic temperatures along the streamer axis varies from  $2.2$  to  $3.2 \times 10^6$  K with the peak value at  $2.1 R_{\odot}$ . At all heights above  $1.5 R_{\odot}$  in the streamer, the latitudinal dependence shows that kinetic temperature is peaked near the streamer axis and decreases by  $1 \times 10^6$  K or more within 10 degrees on either side of the streamer axis. A paper to be submitted to the *Astrophysical Journal Letters* is currently in preparation.

Velocity measurements near the streamer are being studied in two ways. Results from a study of Doppler shifts of the line centers of the profiles suggest high outflows at the edge of the streamer and in the south coronal hole. The line-of-sight velocities are as large as  $30 \text{ km s}^{-1}$  which imply even higher radial velocities. The radial coronal velocities can be determined from a Doppler dimming analysis of the HI Ly- $\alpha$  intensities. Preliminary Doppler dimming results show that the HI Ly- $\alpha$  intensity decreases significantly (relative to the white light polarized radiance) as one moves away from the streamer axis toward the south coronal hole. This result implies that there are high outflow velocities at the streamer/coronal hole interface. A detailed and more quantitative analysis of the outflow velocities is in progress.

## **Coronal Mass Ejection Above The West Limb**

Don Hassler, now at the High Altitude Observatory, has been working with the data from orbit 18, in which a CME (observed with the WL coronagraph) passed partially through the field-of-view of the UVCS integrated Ly- $\alpha$  intensity slit. The same region was viewed before the event during orbit 17. The Soft X-ray Telescope on Yohkoh was also observing during this time period and a collaboration has been established with Keith Strong at Lockheed as well as with the Spartan White Light Coronagraph group at GSFC (Dick Fisher and Lika Guhathakurta) to coordinate the analysis of these data sets. A paper discussing the coordinated observations was prepared for the 3rd SOHO Workshop.

## **Preparations For Spartan 201-2**

### **Characterization**

Larry Gardner completed optical alignment checks and the radiometric characterization of the UVCS in preparation for Spartan 201-2 on the STS-64 mission. The following

measurements were performed on the Ly- $\alpha$  profile and intensity channels of the spectrometer: 1) spectrometer entrance slit positions with respect to the critical occulter edge, 2) disk mask aperture position and throughput, 3) flat field measurements for both array detector channels, 4) detector dark count rates, 5) cross-talk from one array detector channel to the other, 6) system radiometric calibration, and 7) wavelength setting. In addition, the vignetting function of the Ly- $\alpha$  telescope mirror was measured.

Just after the 201-1 flight, the wavelength settings for the Ly- $\alpha$  channel were checked and found to have held. Laboratory measurements of the Ly- $\alpha$  channel required the diffraction grating to be moved, therefore, the Ly- $\alpha$  wavelength position had to be re-established.

Larry Gardner and Leonard Strachan completed optical alignment checks and the radiometric characterization of the OVI channel. The following measurements were performed on the OVI  $\lambda 1032$  and  $\lambda 1037$  channel electron multipliers (CEMs): 1) spectrometer entrance slit position relative to occulter edge, 2) detector dark count measurements, 3) cross talk between OVI channels, 4) cross talk from Ly- $\alpha$  channels, 5) system radiometric calibration, and 6) low resolution wavelength check (using three Nitrogen lines). The OVI telescope mirror vignetting function was also determined.

## **Re-Integration Of UVCS With The Spartan 201 Spacecraft**

The re-integration of the UVCS with the Spartan 201 spacecraft in preparation for STS-64 began in mid-October 1993. Shortly after arrival at Goddard, the UVCS and WLC instruments were installed into the Spartan Instrument Carrier which was assembled into the Service Module. The spacecraft had two 43-hour mission simulation tests, the first in December 1993 and the second in February 1994. The UVCS passed both successfully.

The OVI vac-ion pump failed after the spacecraft vibration test in March 1994. After investigating the impact of replacing the pump, it was decided to fly the OVI detector with the pump turned off. To help ensure that an adequate vacuum can be maintained in flight once the OVI door is opened to the vacuum of space, Spartan was launched with a "hard" vacuum inside the detector and the Spartan Instrument Carrier rather than backfilled with dry nitrogen. It is believed that this approach reduces evacuation time by eliminating virtual leaks. A final 43-hour test occurred in March 1994 and no anomalies were observed. In June, the spacecraft was shipped to KSC to begin the activities for integrating with the STS.

In summary, the results of the laboratory calibration at SAO and environmental tests at GSFC show that Spartan/UVCS was in very good condition for its re-flight. (The OVI vac-ion pump will be replaced before the third flight.) The telescope mechanisms, electronics, and detectors were working well. The optical alignments of the instrument were stable.

## Observing Program For Spartan 201-2

The Spartan/UVCS observing program was modified to optimize the coordinated science data to be obtained during the Ulysses south polar passage. Two of the coronal hole radial scans were extended out to  $3.5 R_{\odot}$  to include Ly- $\alpha$  profile and intensity measurements at 1.5, 1.8, 2.1, 2.5, 3.0 and  $3.5 R_{\odot}$ . Previously, there were no position angles with this complete coverage but the results from the first flight showed that good statistics were achievable in a coronal hole even at the outer heights.

The additional coronal hole observations required the use of 1.5 orbits previously used for streamer observations. This reduction does not affect extensive coverage over the streamer that borders the south polar hole. The streamers are much brighter than coronal holes and therefore they can be sampled with many more observations of shorter duration during a prescribed amount of time.

Another modification concerns the use of the OVI detector. Because, for STS-64 it operated with its vacuum pump turned off, there was a small possibility that the detector might arc when the detector high voltage is turned on. To minimize this risk, the OVI detector was not operated until 14 hours into the mission (to allow time for outgassing once its vacuum door was opened). It was turned on for six orbits during the remainder of the flight.

The number of geocoronal observations programmed for the Spartan 201-2 was unchanged from Spartan 201-1. These observations are made when Spartan is in the Earth's umbra and pointed  $95^{\circ}$ ,  $110^{\circ}$ ,  $140^{\circ}$ ,  $150^{\circ}$ , and  $160^{\circ}$  away from the Sun.

## Preliminary Results From Spartan 201-2

Spartan 201-2 was deployed from the space shuttle on 13 September 1994 and spent about 40 hours observing the extended solar corona. The primary target for this flight was the south polar coronal hole, which was observed for 10 orbits. In addition, observations were made of the boundary between the south coronal hole and a streamer off the southwest limb and the streamer itself. For comparison and in preparation for Spartan 201-3, observations were made of the north polar coronal hole. It was also planned to observe a streamer off the east limb bounding the south coronal hole. Since the only streamer that was visible in the ground based data off the east limb was in the northeast quadrant, and since the pre-programmed observation was only suitable for a streamer, it was decided to observe it as well. Spatial elements observed by the Spartan Ultraviolet Coronal Spectrometer are illustrated in Figure 3. In addition to the coronal observations, center to limb scans were made at position angles between  $-1^{\circ}$  and  $43^{\circ}$  for the HI Ly- $\alpha$  profile, and between  $325^{\circ}$  and  $327^{\circ}$  for the OVI intensity. There also were measurements of the HI Ly- $\alpha$  geocorona at five orientations between  $95$  and  $160$  degrees from the Sun-center axis. Background measurements were made

while the instrument was in the Earth's umbra and while it was facing the Earth's surface. Observations of the intensities of Fe XII  $\lambda 1242A$ , NV  $\lambda 1238$  and MgVI  $\lambda 1192$  were also made.

The observations were fully successful. Observations of HI Ly- $\alpha$ , OVI  $\lambda 1032$  and  $\lambda 1037$ , Fe XII  $\lambda 1242$ , NV  $\lambda 1238$  and possibly Mg VI  $\lambda 1192$  were all obtained. The statistical accuracy for the HI Ly- $\alpha$  line profiles was excellent for both the streamers and the coronal holes. The OVI observations appear to be affected by atmospheric absorption. Atmospheric models are being used to explain and remove the atmospheric effects from the coronal data.

The HI Ly- $\alpha$  profiles and intensities and the O VI intensities appear to be similar to those observed in similar structures on Spartan 201-1. In particular, the HI Ly- $\alpha$  profiles in the coronal holes have complex shapes as they did in the first flight. However, the detailed shapes are different in the two cases.

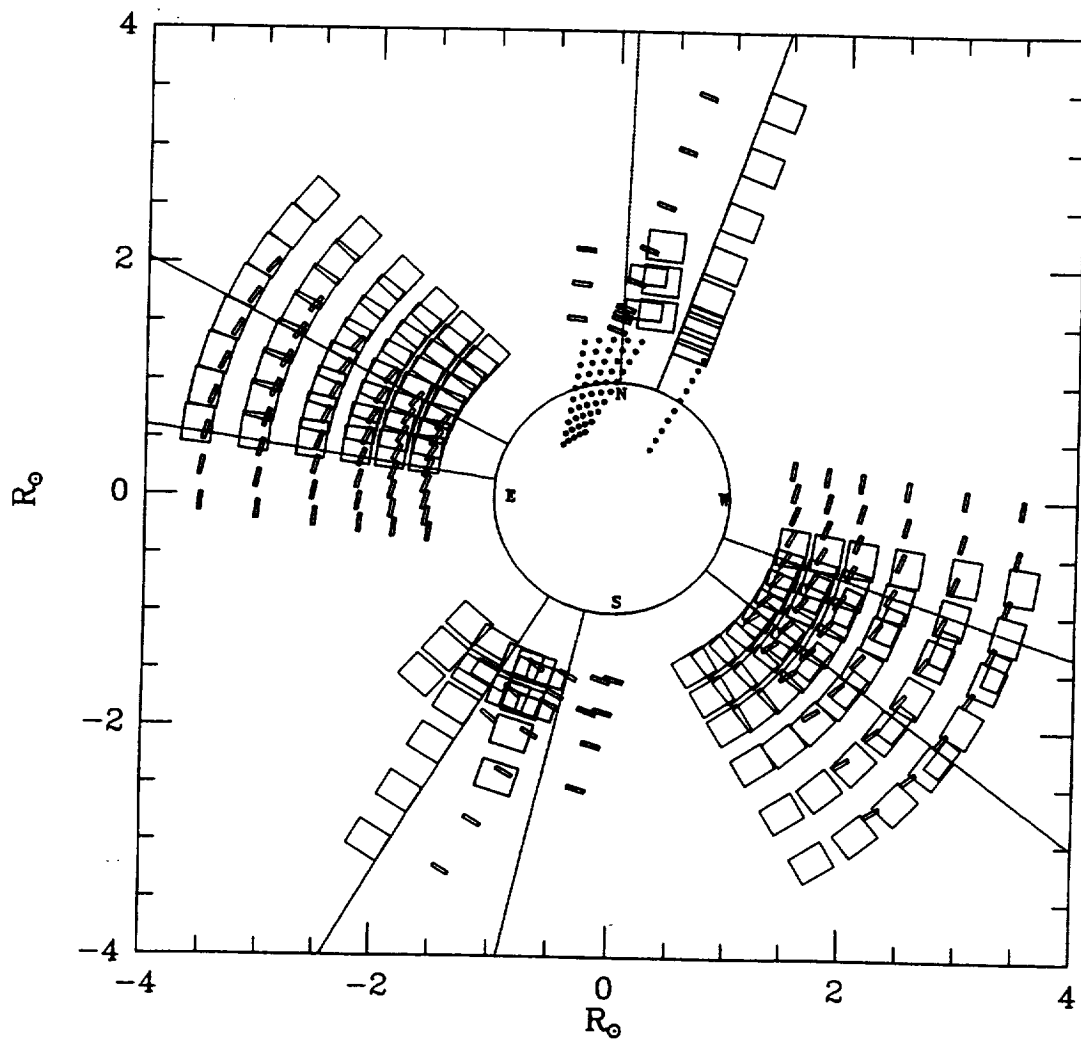


Figure 3: Spartan 201-2: All UVCS Observations